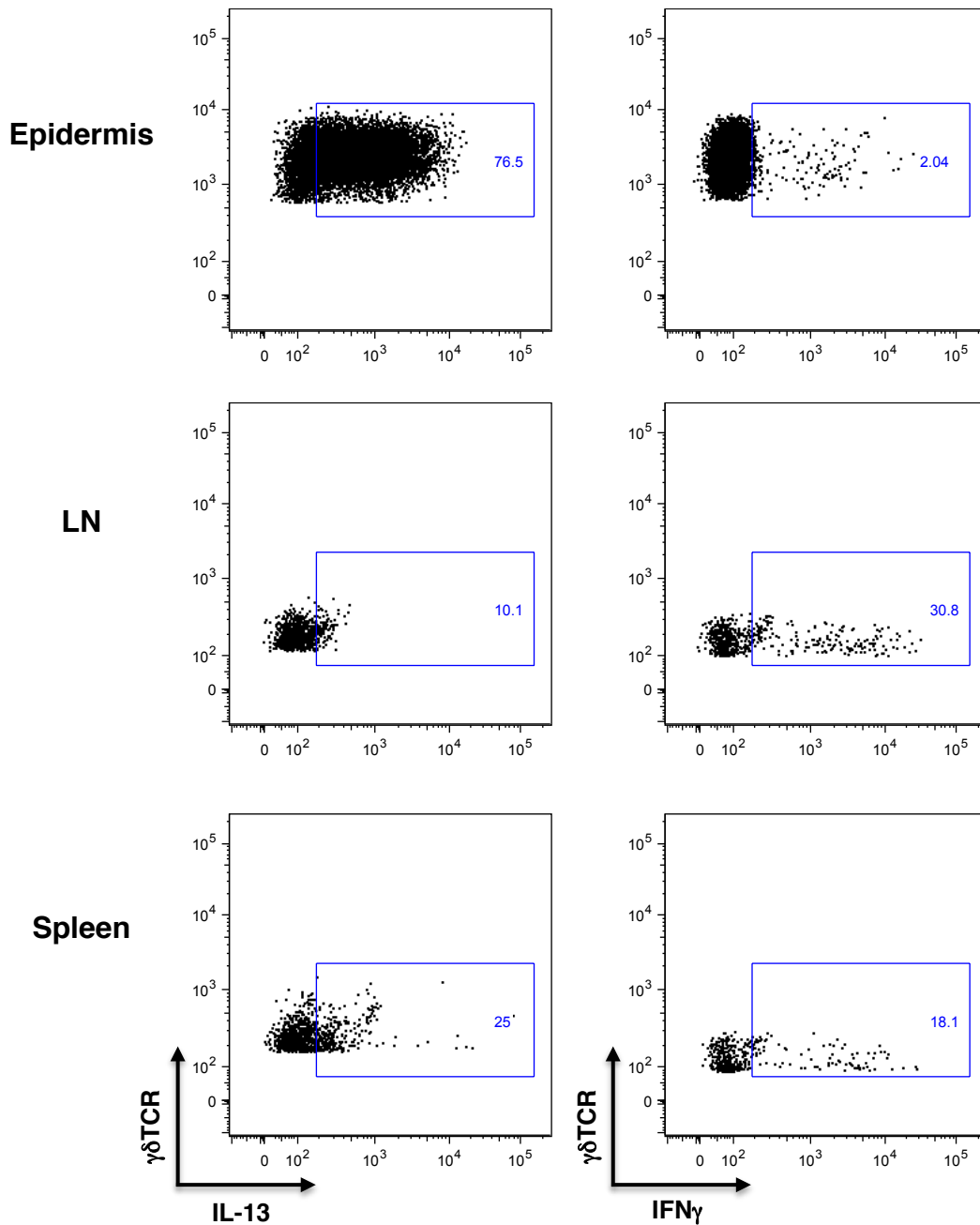


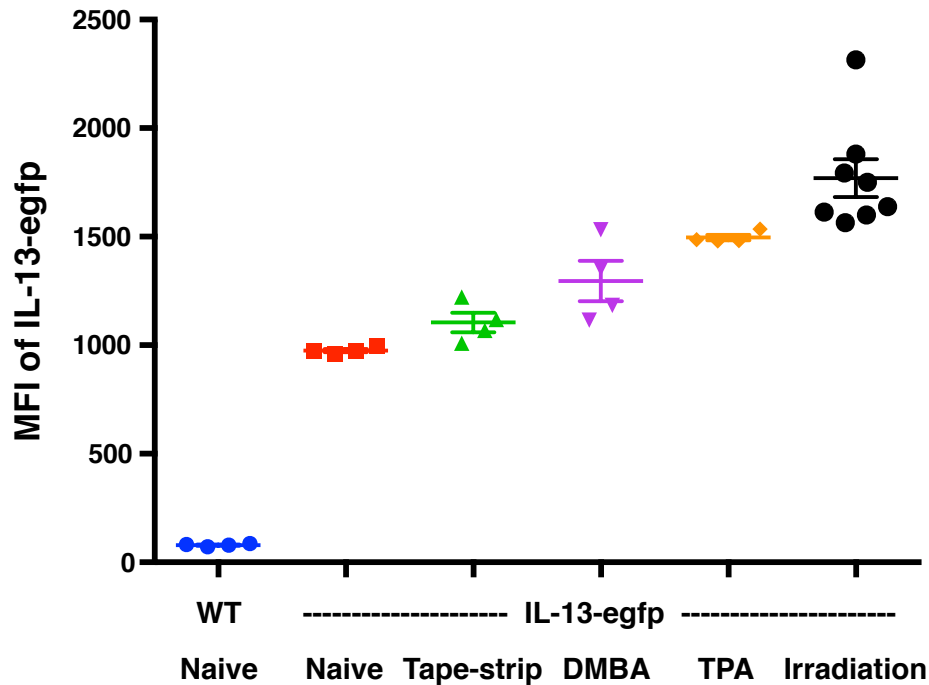
**Supplementary Figure 1. Epidermal IELs are responsive to topical environmental challenge**

Confocal microscopy of IELs examining their morphology *in situ* in epidermal sheets freshly isolated from the ear of FVB WT mice (from left to right) untreated, abraded by tape-stripping, exposed topically to TPA or DMBA. Epidermis was isolated 24h after skin challenge and skin IELs visualized with V $\gamma$ 5 TCR ab (green). Representative images are shown. Original magnification x40. Scale bars = 50 $\mu$ m.



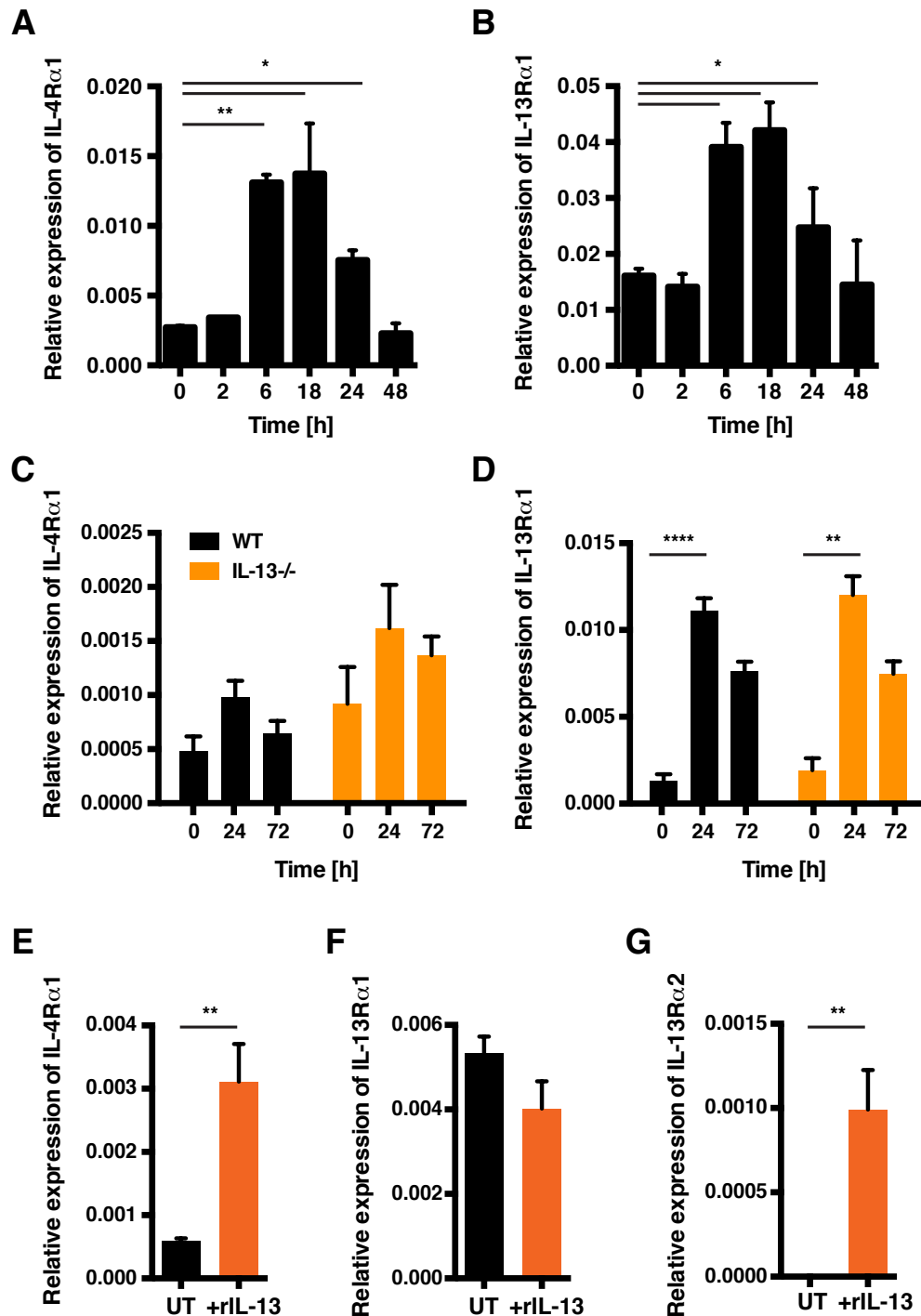
**Supplementary Figure 2. Epidermal  $\gamma\delta$  T cells are uniquely biased towards IL-13 production**

IL-13 and IFN $\gamma$  production by  $\gamma\delta$  T cells isolated from the epidermis, skin draining lymph node (LN) and spleen from the same FVB WT animal was analysed following 4h *in vitro* stimulation with PMA/ionomycin. Cells were stained and gated on the  $\gamma\delta$ TCR and intracellular levels of IL-13 and IFN $\gamma$  assessed by FACS. Cytokine positive cells were defined using isotype control gating. Representative examples are shown.



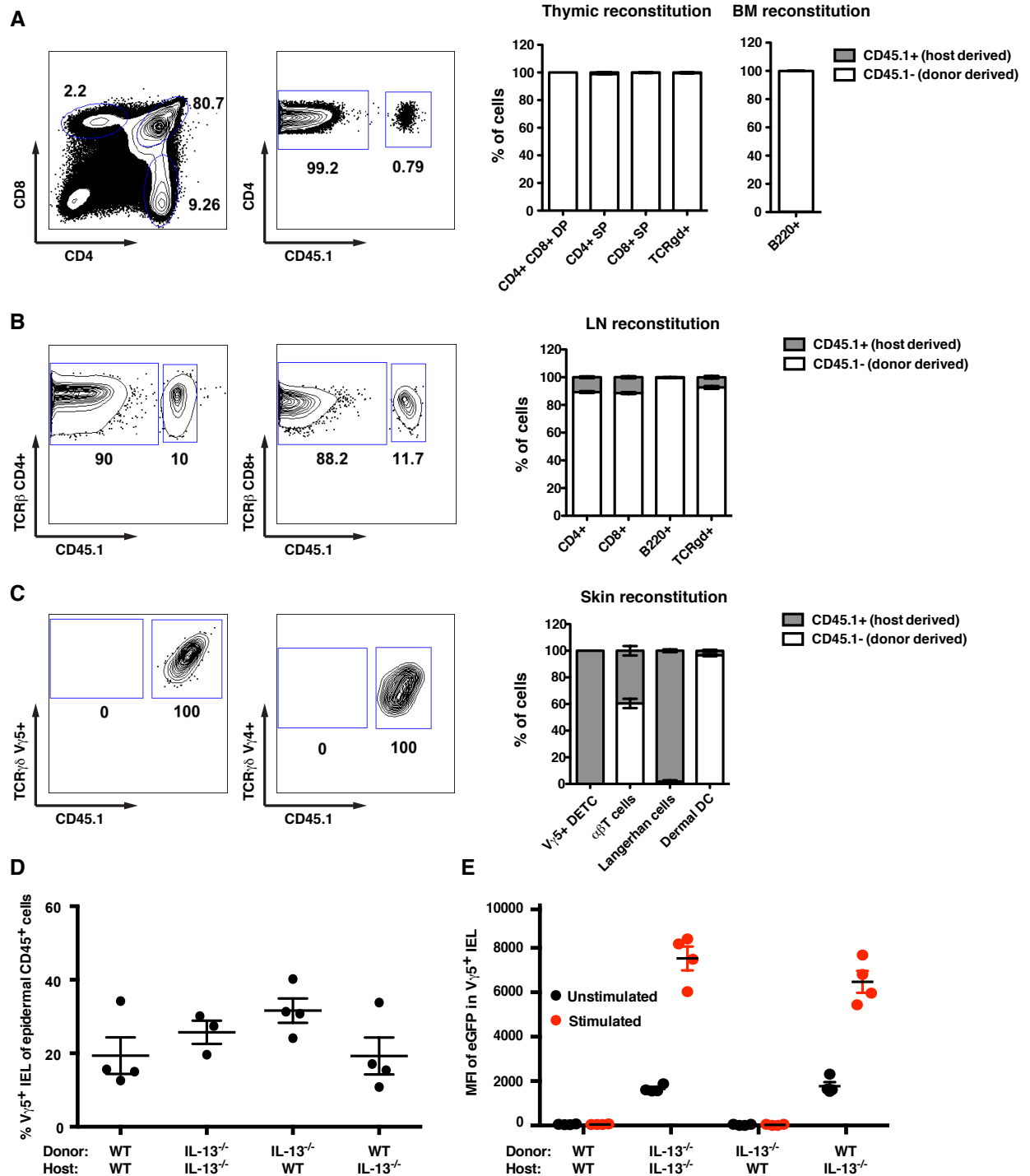
**Supplementary Figure 3. Epidermal IELs express IL-13 in resting skin and upregulate expression further following challenge**

Skin  $\gamma\delta$  T cells were isolated from resting naïve WT BALB/c and IL-13-egfp reporter mice as well as from IL-13-egfp mice following challenge by topical abrasion (tape-stripping), topical exposure to the carcinogen DMBA or to TPA and following whole body irradiation (750 Rads). IL-13-egfp MFI was subsequently assessed by FACS (n=4-8 per group). All epidermal  $\gamma\delta$  TCR<sup>+</sup> IELs were positive for IL-13-egfp already at resting state (100%) with a mean MFI of 975. The mean IEL egfp MFI was further enhanced following challenge (p<0.05 for tape-stripping and DMBA, p<0.0001 for TPA and irradiation). All dermal  $\gamma\delta$  T cells remained egfp negative throughout.



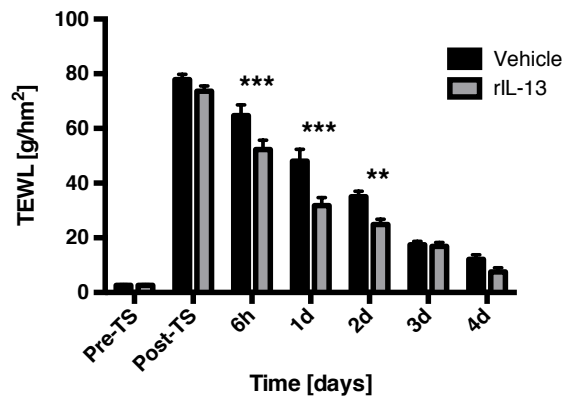
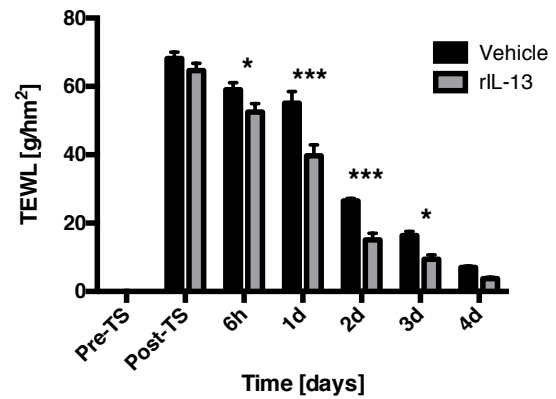
#### Supplementary Figure 4. IL-13R expression is stress-regulated on KCs

Quantitative RT-PCR analysis of (A) IL-4 $\alpha$ R1 and (B) IL-13 $\alpha$ R1 mRNA in isolated FVB WT epidermis at the indicated time-points after skin abrasion by tape-stripping (n=3 per time-point). (C-D) Expression of IL-4 $\alpha$ R1 and IL-13 $\alpha$ R1 mRNA in epidermis of BALB/c WT and IL-13 $^{-/-}$  mice at indicated time-points after a single skin exposure to DMBA (n=4 per time-point). (E-G) Primary neonatal KCs grown *in vitro* were assessed for expression of (E) IL-4 $\alpha$ R1, (F) IL-13 $\alpha$ R1 and (G) IL-13 $\alpha$ R2 receptor with/without stimulation by 20 ng/ml rIL-13 (n=6). UT = untreated. Data in (A-C) was done by qRT-PCR and are expressed as mean  $\pm$  1 SEM relative to the control gene cyclophylin. BALB/c WT mice are shown in black bars, IL-13 $^{-/-}$  mice in orange bars. Statistical significance of difference between experimental groups was determined using Student's t-test for unpaired data with \* correlating to p<0.05, \*\* p<0.01, \*\*\* p<0.001 and \*\*\*\* p<0.0001.



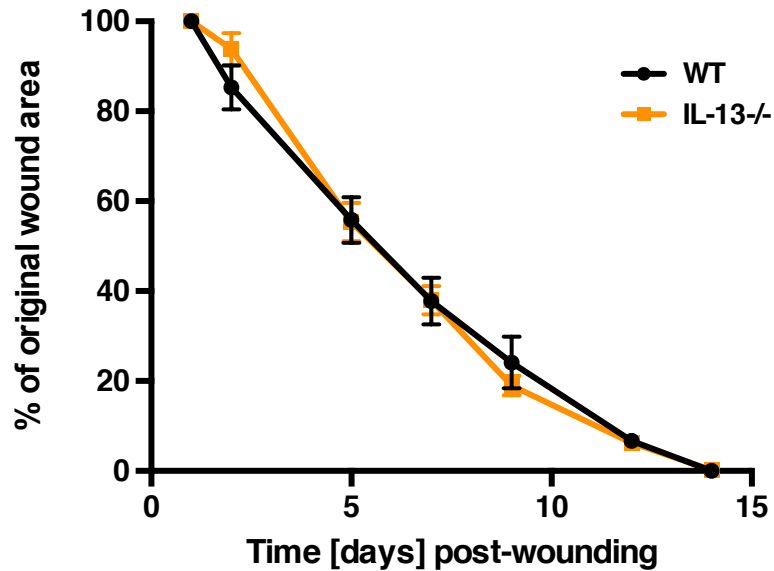
### Supplementary Figure 5. IL-13-sufficient or IL-13-deficient IELs are created by BM chimerism

(A-C) CD45.1<sup>+</sup> host mice were full-body radiated at 750rads and immediately transplanted with CD45.1<sup>-</sup> donor bone marrow (BM). 8 weeks after the BM transplant organs and tissues were analysed for host (CD45.1<sup>+</sup>) cells versus donor (CD45.1<sup>-</sup>) cells in (A) thymus and BM B cells, (B) peripheral LN and (C) skin. (D-E) BALB/c WT/IL-13<sup>-/-</sup> BM chimeras were created by reconstituting irradiated WT mice with BM from mice in which both IL-13 alleles had been replaced by egfp (IL-13<sup>egfp/egfp</sup>→WT). (For brevity IL-13<sup>egfp/egfp</sup> mice are termed IL-13<sup>-/-</sup> henceforth). As controls, irradiated IL-13<sup>-/-</sup> mice were reconstituted with WT BM (WT→IL-13<sup>-/-</sup>), WT mice reconstituted with WT BM (WT→WT) and IL-13<sup>-/-</sup> mice reconstituted with IL-13<sup>-/-</sup> BM (IL-13<sup>-/-</sup>→IL-13<sup>-/-</sup>). (D) Number of Vγ5<sup>+</sup> skin IELs were assessed in the epidermis 8 weeks after reconstitution and (E) their egfp signal assessed by flow cytometry at resting or following *ex vivo* stimulation with PMA/iono (n=4 per group). IL-13<sup>-/-</sup> donor to WT have IL-13-sufficient IELs; WT donor to IL-13<sup>-/-</sup> host have IL-13-deficient IELs.

**A****B**

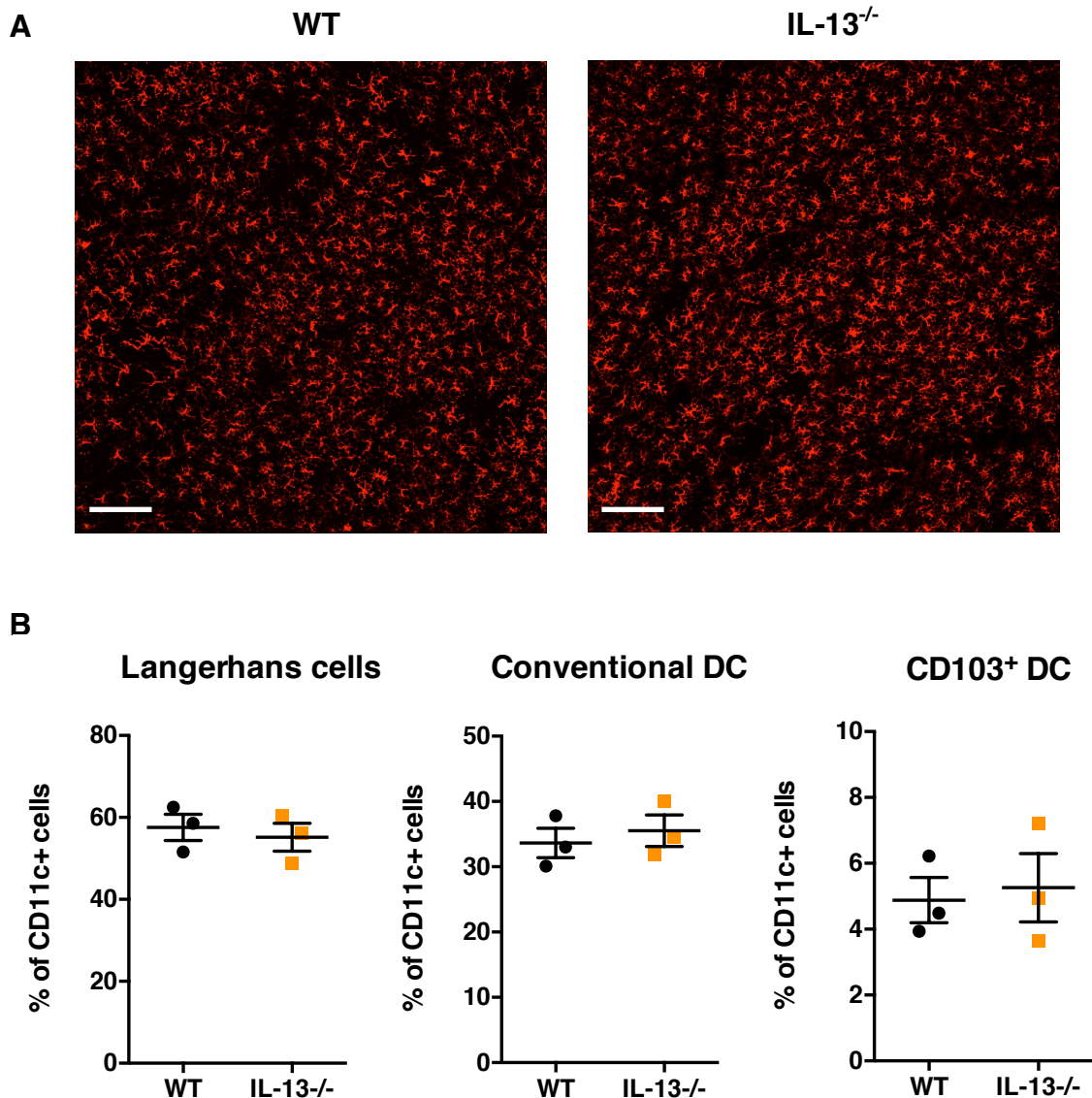
### Supplementary Figure 6. rIL-13 administered topically enhances speed of barrier recovery

TEWL was measured on the dorsal ear before and at various times after skin abrasion by tape-stripping (TS) (6x). (A) FVB WT mice were treated topically with 50ng rIL-13 just after tape-stripping and again after 24h and compared to mice treated with vehicle only (PBS) (n=10 per group). (B) BALB/c WT mice were treated topically with 50ng rIL-13 just after tape-stripping and again after 24h and compared to mice treated with vehicle only (n=8 per group). Statistical significance of difference between experimental groups was determined using Student's t-test for unpaired data with \* correlating to  $p < 0.05$ , \*\*  $p < 0.01$  and \*\*\*  $p < 0.001$ .



**Supplementary Figure 7. IL-13 is redundant for full skin thickness wound healing**

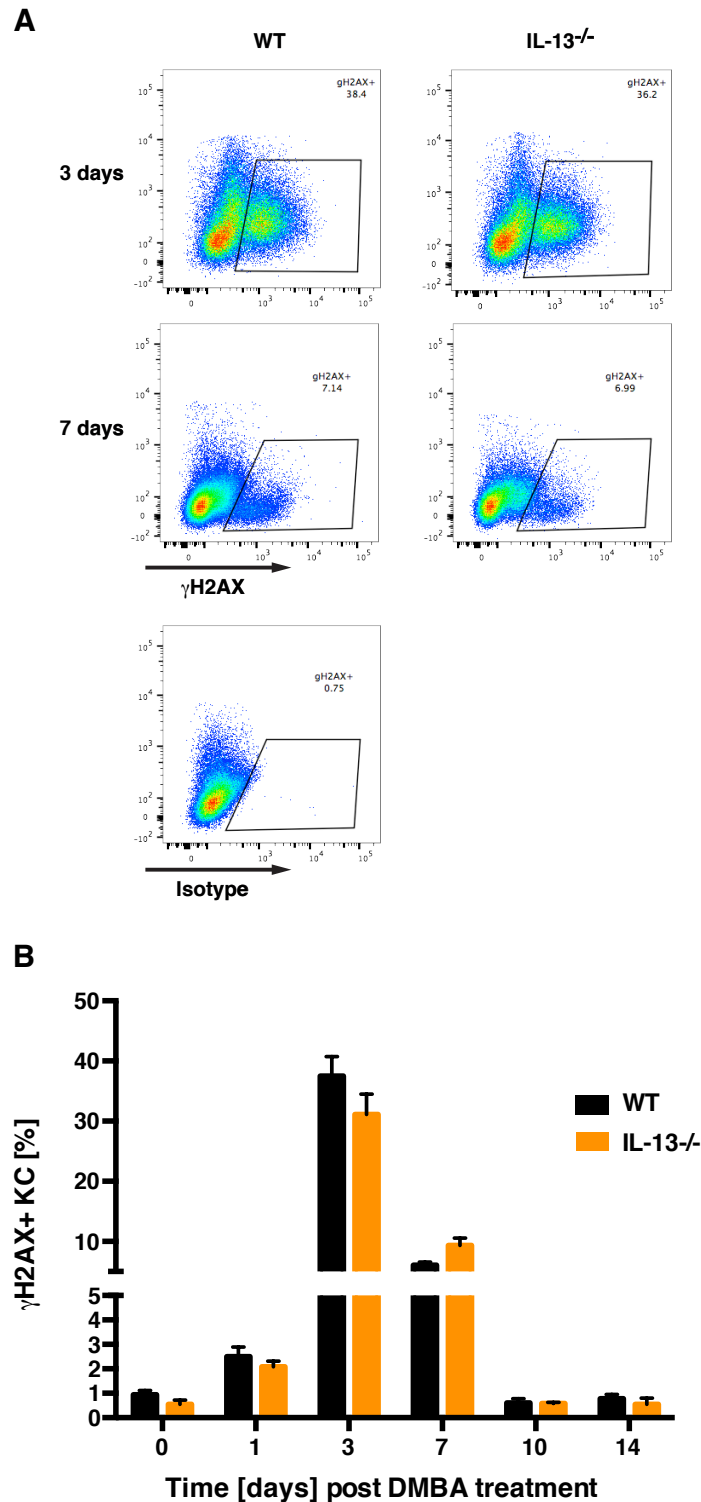
A full skin thickness, 0.5 mm punch biopsy, wound was made on the lower back of BALB/c WT and IL-13<sup>-/-</sup> mice and wound closure assessed over time. Wound sizes were measured with calipers daily for the first 2 days, and then once every 2 days until complete wound closure. The wound sagittal (x) and transverse (y) plane was measured and these were applied to the ellipse area formula to calculate wound area: (area =  $\pi$  (radius x)(radius y)). Data is shown as mean % of the original wound area at day 0  $\pm$  1 SEM (n=8 per group).



**Supplementary Figure 8. Absence of IL-13 does not alter Langerhans cell networks or skin dendritic cell numbers**

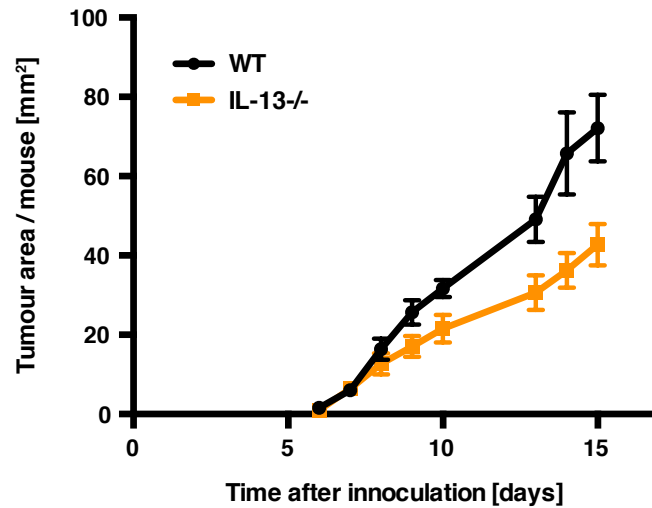
Naïve BALB/c WT and IL-13<sup>-/-</sup> mice were analysed for presence of Langerhans cells and dermal DC populations. (A) Epidermal sheets were collected and stained freshly for Langerin<sup>+</sup> (red) cell networks. Epidermal sheets were analysed on a Leica Sp5 fluorescence microscope. 3 mice were analysed per group; a representative example of each group is shown. Original magnification x20. Scale bars = 100µm. (B) Whole skin was isolated and single cell suspensions were analysed by FACS for numbers of Langerhans cells (gated as CD45<sup>+</sup>, CD64<sup>-</sup>, CD11c<sup>+</sup>, CD11b<sup>mid</sup>, Langerin<sup>+</sup>), conventional DC (gated as CD45<sup>+</sup>, CD64<sup>-</sup>, CD11c<sup>+</sup>, CD11b<sup>hi</sup>, Langerin<sup>-</sup>) and CD103<sup>+</sup> DC (gated as CD45<sup>+</sup>, CD64<sup>-</sup>, CD11c<sup>+</sup>, CD11b<sup>lo</sup>, Langerin<sup>+</sup>, CD103<sup>+</sup>, XCR1<sup>+</sup>) (n=3 per group). Data is represented as % of total CD11c<sup>+</sup> DC population.





### Supplementary Figure 9. Topical DMBA exposure induces similar level of EC DNA-damage in the absence of IL-13

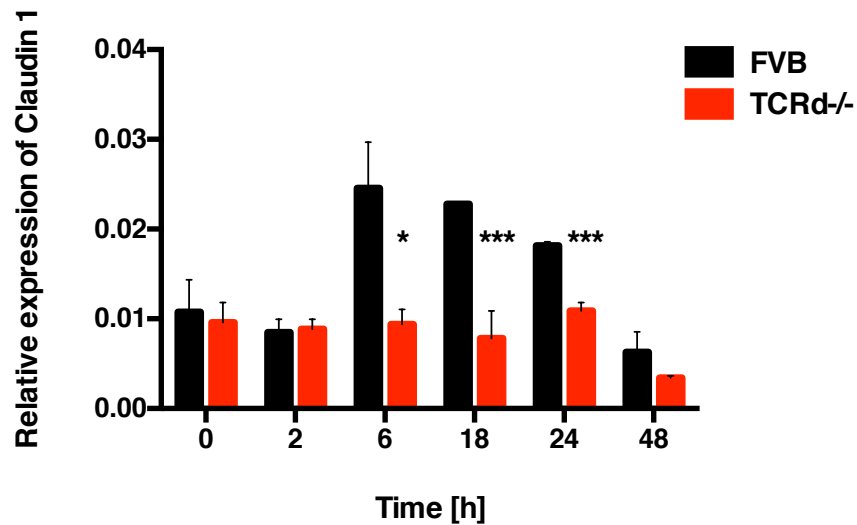
BALB/c WT and IL-13<sup>-/-</sup> mice were treated with a single dose of 200nmol DMBA on the dorsal ear skin. At selected time-points thereafter epidermis was isolated and CD45<sup>-</sup> KC stained for intranuclear  $\gamma$ H2AX.  $\gamma$ H2AX (the phosphorylation of the histone H2AX) flanks sites of double-stranded DNA breaks caused by the DMBA exposure.  $\gamma$ H2AX is a sensitive marker for quantification of DNA-damage and repair processes. Dead cells were excluded from the analysis using a dead cell dye. (A) Representative staining of  $\gamma$ H2AX at peak time-points with isotype control. (B) Quantification of % KC that have phosphorylated H2AX at varying time-points following DMBA in BALB/c WT (black bars) and IL-13<sup>-/-</sup> (orange bars) mice (n=3-14 mice per group per time-point). Data is represented as mean  $\pm$  1 SEM.



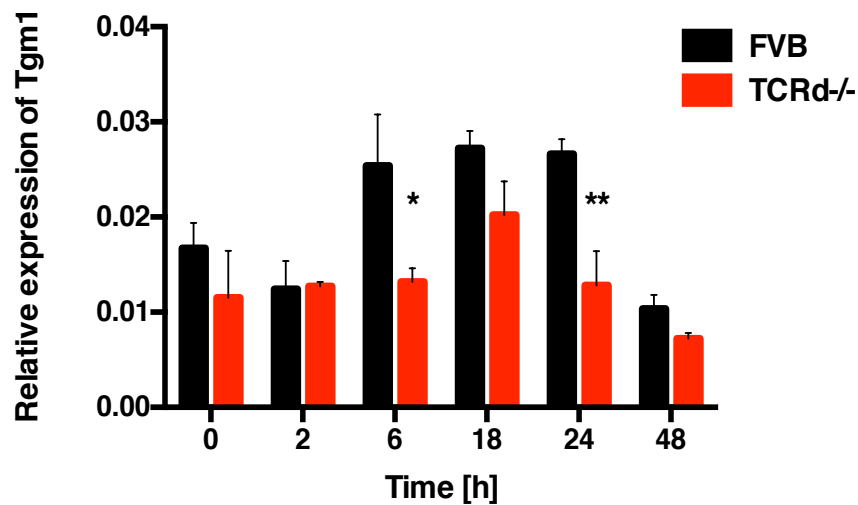
**Supplementary Figure 10. The tumour protective effect of IL-13 is restricted to carcinogenesis at the epithelial skin barrier**

BALB/c WT and IL-13<sup>-/-</sup> mice were inoculated subcutaneously in the flank with  $10^4$  CT26 cells and tumour growth measured over time. Tumour sizes were measured with calipers daily and the data shown as the average tumour area per mouse over time (n=7 per group).

**A**

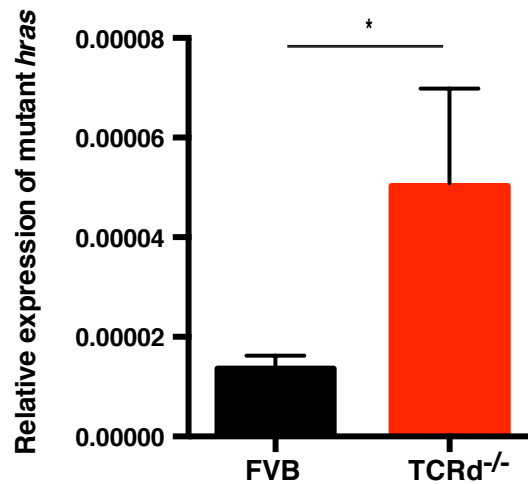


**B**



**Supplementary Figure 11. IELs promote epithelial maturation following tape-stripping**

Expression analysis of (A) claudin 1 and (B) transglutaminase 1 in isolated epidermis from FVB WT mice (black bars) and TCRd<sup>-/-</sup> mice (red bars) at indicated time-points after skin abrasion by tape-stripping (n=3 per time-point). Data was done by qRT-PCR and are expressed as mean  $\pm$  1 SEM relative to the control gene cyclophylin. Statistical significance of difference between experimental groups was determined using Student's t-test for unpaired data with \* correlating to  $p < 0.05$ , \*\*  $p < 0.01$  and \*\*\*  $p < 0.001$ .



**Supplementary Figure 12. In the absence of IELs *hras* mutations accumulate in the epidermis**

FVB WT mice and TCRd<sup>-/-</sup> mice were treated with 200nmol DMBA on back skin once weekly for 6 weeks. Mice had no clinically apparent disease at this point. Epidermis was then collected and total genomic DNA extracted. A custom Taqman qRT-PCR assay for mutant *hras* (A->T transversion within *hras* codon 61) was performed and expression normalised against *Actb* (n=5 per group). Data is represented as mean  $\pm$  1 SEM. Statistical significance of difference between experimental groups was determined using Student's t-test for unpaired data with \* correlating to p<0.05.